Synthesis and Characterization of Highly Efficient Photorefractive Polymer Composites with Long Phase Stability

E. Hendrickx, J. F. Wang, J. L. Maldonado, B. L. Volodin, Sandalphon, E. A. Mash,† A. Persoons, B. Kippelen,* and N. Peyghambarian*

The University of Arizona, Optical Sciences Center, Tucson, Arizona 85721
The University of Arizona, Department of Chemistry, Tucson, Arizona 85721

Received October 7, 1997; Revised Manuscript Received November 17, 1997

ABSTRACT: We have synthesized the chromophores 4-[(4′-nitrophenyl)azo]-1,3-bis[(3″- or 4″-vinylbenzyl)-oxy]benzene (NPADVBB) and 4-[(4′-nitrophenyl)azo]-1,3-bis(benzyloxy)benzene (NPADB). New polymer composites based on the photoconductor poly(9-vinylcarbazole), the plasticizer 9-ethylcarbazole, NPADVBB, and the sensitizers 2,4,7-trinitro-9-fluorenone and (2,4,7-trinitro-9-fluorenylidene)malonitrile were prepared. Ellipsometric measurements and degenerate four-wave mixing experiments were performed at 633 and 830 nm. The composites showed excellent phase stability, and nearly complete diffraction was observed at 633 nm. The two-beam coupling gain was limited by the small phase shift between the interference pattern and the index grating.

I . INTRODUCTION

In photorefractive materials, the absorption of light, followed by diffusion and drift of the free charges, generates a space-charge field that modulates the refractive index.[1] Research performed on these materials during the past decades has shown that they can be used for optical storage, exchange, and manipulation of large amounts of information.[2] For 30 years, the main photorefractive materials available have been inorganic crystals such as $LiNbO_3$ and $BaTiO_3$, and their high cost has hindered the development of photorefractive devices. It is now firmly established that the photorefractive effect can also be observed in organic materials, such as polymer films,[3] liquid crystals,[4] and organic glasses.[5] During the past years, the photorefractive efficiency of these organic materials has improved dramatically, and it now exceeds that of the traditional inorganic crystals. Since organic materials combine ease of processing, low cost, high efficiency, and flexibility, they are the materials of choice for many device applications.

One of the most efficient materials reported so far is a plasticized guest−host polymer with a glass transition temperature T_g below room temperature.[6] This material is made of the photoconductor poly(9-vinylcarbazole) (PVK), the plasticizer 9-ethylcarbazole (ECZ), the nonlinear optical chromophore 2,5-dimethyl-4-(*p*-nitrophenyl)azoanisole (DMNPAA), and the sensitizer 2,4,7-trinitro-9-fluorenone (TNF), which forms a charge-transfer complex with the carbazole moieties. If a periodic light-intensity pattern is incident on the material, charges are generated in the bright regions due to the optical excitation of the charge-transfer complex. Since the carbazole units act as hole-transport agents and only 2 wt % of TNF is present, the holes are free to move to the dark regions of the grating by diffusion or drift under the influence of an applied external field. In traditional photorefractive materials, the space charge field that is produced by this inhomogeneous charge distribution then modulates the refractive index through the electro-optic effect. If the material has a T_g below room temperature, the index modulation amplitude is further enhanced by birefringence.[7] This guest−host polymer was shown to combine nearly 100% diffraction efficiency in 105-μm-thick samples, subsecond response time (500 ms), and high resolution ($<3\ \mu$m). The main disadvantage of the material lies in the mutual incompatibility of the polar dye DMNPAA and the nonpolar, plasticized polymer matrix, which leads to phase separation, through a nucleation and growth mechanism, as the polar dye slowly crystallizes.[8] These crystallites scatter light strongly, reduce the dielectric strength of the material, and consequently limit the sample lifetime. The speed of phase separation was found to be controlled by the speed of diffusion of the polar dyes in the polymer matrix, and typically samples with 40 wt % DMNPAA in a matrix of PVK/ECZ in a 2/1 ratio are stable for several months at room temperature. It has been shown that the sample lifetime can be improved by a factor of 5 by using a eutectic mixture of 2,5- and 3,5-DMNPAA without loss of photorefractive efficiency.[9] If dyes with a melting point below room temperature are used, the phase stability also improves, but at the cost of lower efficiency.[10] In previous work, we have shown that the sample lifetime can be improved by two orders of magnitude, without loss of efficiency, if DMNPAA is substituted by the chromophore 4-[(4′-nitrophenyl)azo]-1,3-bis[(3″- or 4″-vinylbenzyl)oxy]benzene (NPADVBB).[8]

Here, we describe the synthesis and characterization of NPADVBB and a structurally similar dye, 4-[(4′-nitrophenyl)azo]-1,3-bis(benzyloxy)benzene (NPADB). We show that by substituting TNF for TNFDM the absorption of the charge-transfer complex is shifted to higher wavelengths, which extends the wavelength range of these materials to 830 nm in the infrared region. We performed ellipsometric measurements and four-wave mixing experiments both at 633 and 830 nm. The internal diffraction efficiency of the material reaches nearly 100% at 633 nm. Two-beam coupling experiments show that the grating is photorefractive but also

* To whom correspondence should be addressed. B.K.: Telephone: (520) 621-4341. Fax: (520) 626-4221. E-mail: kippelen@u.arizona.edu. N.P.: nnp@u.arizona.edu.
† The University of Arizona, Department of Chemistry.

S0024-9297(97)01477-0 CCC: $15.00
Published on Web 01/14/1998

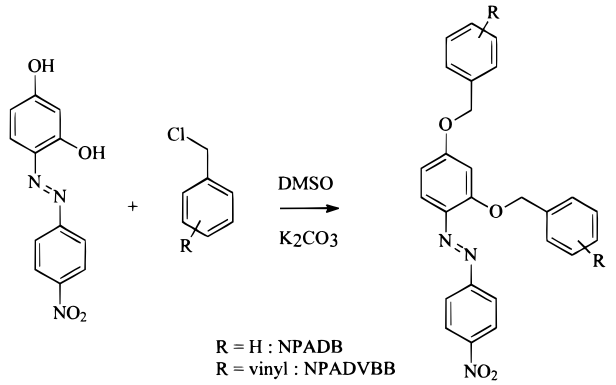

Figure 1. Synthesis of NPADVBB and NPADB.

that the gain coefficient is limited by the small phase shift between the index grating and the intensity pattern.

II. EXPERIMENTAL SECTION

1. Synthesis. The reagents used are tetrahydrofuran (THF), dried and redistilled; methyl sulfoxide, 99+% (Aldrich); K_2CO_3, AR (Mallinckrodt); 4-[(4′-nitrophenyl)azo]resorcinol, 90% (Aldrich); benzyl chloride, 99% (Aldrich); and vinylbenzyl chloride, 98% (Aldrich). The ratio of the two isomers in vinylbenzyl chloride was determined from both gas chromatography (58.5% 3-vinylbenzyl chloride and 41.5% 4-vinylbenzyl chloride) and ^{1}H NMR ($CDCl_3$, 500 MHz): δ 4.58 ppm (55.4% 3-vinylbenzyl chloride) and 4.57 ppm (44.6% 4-vinylbenzyl chloride). The NMR instruments used were Gemini-200, Varian; Unity-300, Varian; and AM-500, Bruker.

The reaction scheme is shown in Figure 1. Fifteen grams of 4-[(4′-nitrophenyl)azo]-1,3-benzenediol (commercial name: 4-(4′-nitrophenyl)azoresorcinol), 18.0 mL of vinylbenzyl chloride, 16 g of K_2CO_3, and 250 mL of THF were mixed in a 500-mL round-bottomed flask, fitted with a condenser, and refluxed for 24 h. Thin layer chromatography (TLC) showed that only a small amount of reaction product was formed under these conditions. Methyl sulfoxide (100 mL) was added, and the mixture was kept at reflux. The color of the solution turned from red into dark red. TLC indicated that the reaction was complete within 3 h. THF was removed on a rotary evaporator, and the solution was poured into a 500-mL ice/water mixture. The orange-red precipitate was collected by filtration and purified by chromatography on silica gel eluted with toluene (R_f = 0.6). The compound (yield 78.9%, 20.2 g) was recrystallized from a mixture of acetonitrile (100 mL) and toluene (20 mL).

The melting point of NPADVBB falls in the range 122−134 °C. Assuming equal reactivity for the different vinylbenzyl isomers, NPADVBB is a 19.9% (4″, 4″), 24.7% (4″, 3″), 24.7% (3″, 4″), and 30.7% (3″, 3″) isomeric mixture (41.5% in 4″-position and 58.5% in 3″-position). Integrated ^{13}C NMR ($CDCl_3$, 125 MHz) for peaks at 71.3, 71.2, 70.3, and 70.2 shows that the ratios are 21.1%, 20.5%, 24.5%, and 33.9% (45.6% in 4″-position and 54.4% in 3″-position), close to the isomer distribution for equal reactivity. Anal. Calcd for $C_{30}H_{25}N_3O_4$: C, 73.32; H, 5.09; N, 8.55. Found: C, 73.33; H, 5.09; N, 8.41. MS (*m*/*e*) 492.0 (M^+, 100%). ^{1}H ($CDCl_3$, 200 MHz) δ: 8.31 (dd, J = 8.8 Hz, J = 1.8 Hz, 2 H), 7.94 (dd, J = 9.0 Hz, J = 1.8 Hz, 2 H), 7.80 (d, J = 9.0 Hz, 1 H), 7.57−7.32 (m, 10 H), 6.80−6.63 (m, 4 H), 5.77 (d, J = 17.6 Hz, 2 H), 5.31−5.25 (s + d, J = 11 Hz, 4 H), 5.08 (s, 2 H). ^{13}C ($CDCl_3$, 50 MHz) δ: 164.0, 163.9, 159.0, 158.9, 156.5, 148.0, 137.9, 137.7, 137.4, 136.8, 136.5, 136.4, 136.3, 136.2, 136.2, 135.9, 135.4, 128.9, 128.8, 127.7, 127.3, 126.9, 126.5, 126.4, 126.3, 126.1, 125.9, 125.4, 124.6, 123.1, 118.3, 114.5, 114.4, 114.3, 114.2, 107.7, 107.6, 101.9, 71.3, 71.2, 70.3, 70.2.

NPADB was synthesized using a procedure similar to that for NPADVBB, but without using THF. Mp: 148.5−149.0 °C. Anal. Calcd for $C_{26}H_{21}N_3O_4$: C, 71.06; H, 4.82; N, 9.56. Found: C, 71.10; H, 5.00; N, 9.53. ^{1}H NMR ($CDCl_3$, 300 MHz) δ: 8.33 (dd, J = 6.9 Hz, J = 2.1 Hz, 2 H), 7.95 (dd, J = 6.9 Hz, J = 2.1 Hz, 2 H), 7.81 (d, J = 9.3 Hz, 1 H), 7.50−7.34 (m, 10 H), 6.72 (d, J = 2.4 Hz, 1 H), 6.66 (dd, J = 9.0 Hz, J = 2.4 Hz, 1 H), 5.30 (s, 2 H), 5.10 (s, 2 H). ^{13}C ($CDCl_3$, 75 MHz) δ: 164.0 (C), 159.0 (C), 156.5 (C), 147.9 (C), 137.4 (C), 136.5 (C), 135.9 (C), 128.7 (CH), 128.6 (CH), 128.3 (CH), 128.0 (CH), 127.5 (CH), 127.0 (CH), 124.7 (CH), 123.1 (CH), 118.4 (CH), 107.7 (CH), 101.9 (CH), 71.5 (CH_2), 70.4 (CH_2).

2. Sample Preparation and Sample Stability. PVK was purchased from Aldrich (average M_w ca. 1 100 000. T_g 200 °C) and purified by dripping 400 mL of a 5 wt % solution of PVK in CH_2Cl_2 in 1600 mL of methanol while stirring. ECZ (Aldrich) was purified by recrystallization from ethanol. (mp after purification is 70 °C). TNF (Aldrich) and TNFDM (Aldrich) were used without further purification.

Samples were prepared by dissolving PVK, ECZ, NPADVBB, NPADB, TNF, or TNFDM in 10−15 mL of $CHCl_3$. The solution was filtered through an Acrodisc filter with a PTFE membrane of 0.2-μm pore size, and the solvent was evaporated with a rotary evaporator. The mixture was dried for 2 h in a vacuum oven at 75 °C and 1000 Pa. Next, the dried material was heated up to 150 °C, mixed mechanically between two glass slides, and cooled down rapidly by putting the glass slides on a metal plate at room temperature. This step was repeated for four or five times until the mixture was homogeneous and almost free from trapped air bubbles. A small piece of this material was pressed between two ITO-covered glass slides at 150 °C and again cooled down rapidly to room temperature. Glass spacers were used to ensure a uniform sample thickness of 105 μm. Finally, to protect the samples from moisture, they were encapsulated with quick setting epoxy adhesive. The NPADVBB-based samples had composition NPADVBB/PVK/ECZ/TNF 39/39/20/2 wt % (NPADVBB-I) and NPADVBB/PVK/ECZ/TNFDM 39/39/20/2 wt % (NPADVBB-II).

A shortcoming of previously reported photorefractive polymer composites was their thermal stability. NPADVBB has a molecular structure that is similar to that of NPADB, but its melting point is lower because it is an isomeric mixture. In a previous study we have shown that composites with NPADVBB (39 wt % NPADVBB; PVK/ECZ 2/1) are stable for 110 min at 85 °C, whereas composites with NPADB (39 wt % NPADB; PVK/ECZ 2/1) crystallize after 2.3 min at 85 °C.[8] The NPADVBB-based composites have been used for 1 year at room temperature under various applied field conditions (up to 50 V μm^{-1} for several hours) and showed only minor changes in external diffraction efficiency. This clearly shows the effectiveness of using isomeric dye mixtures to prevent sample crystallization. Because of the fast crystallization, we did not analyze the photorefractive properties of NPADB-based composites.

A still more effective strategy to prevent crystallization would be to cross-link NPADVBB. However, NPADVBB proved very hard to cross-link at low temperatures (80 °C), even with benzoyl peroxide and azobis(isobutyronitrile) as initiator. At elevated temperature, the pure compound can be polymerized. After heating up to 180 °C for 2 h, only 2% of the solid product could be extracted using acetone (three times), THF (reflux, one time), and DMF (90 °C, two times). Cross-linking of NPADVBB in polymer composites with ECZ and PVK was also observed after 2 h at 180 °C but did not yield samples of good optical quality.

III. Discussion

1. Linear Absorption. To extend the sensitivity of the photorefractive materials to higher wavelengths, we substituted the sensitizer TNF for TNFDM. Just as does TNF, TNFDM forms a charge-transfer complex with the carbazole moieties, but, due to the stronger electron-withdrawing character of the dicyanovinyl group of TNFDM compared to the carbonyl group of TNF, the absorption of the charge-transfer complex is shifted to lower energies. The absorption spectra and

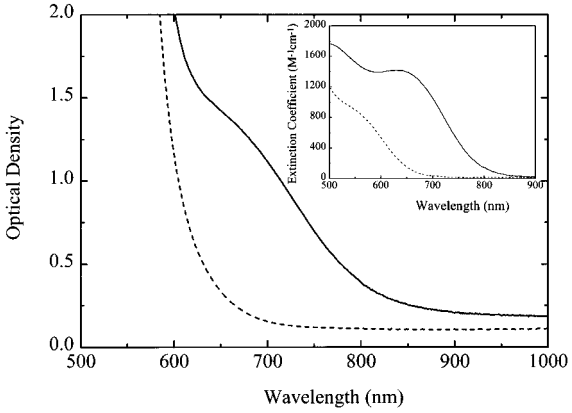

Figure 2. Optical density of NPADVBB/PVK/ECZ/TNF 39/39/20/2 wt % (dashed line) and NPADVBB/PVK/ECZ/TNFDM 39/39/20/2 wt % (full line) polymer composite samples (thickness 105 μm). Inset: Extinction coefficient of the TNF−ECZ (dashed line) and TNFDM−ECZ (full line) charge-transfer spectra in chloroform.

stability constants for the TNFDM−ECZ and TNF−ECZ complexes were determined spectrophotometrically according to the procedure described in ref 11. The linear absorption spectra of the two complexes in chloroform are shown in the inset in Figure 2. The stability constants of the TNF−ECZ complex and the TNFDM−ECZ complex in chloroform were found to be 7.1 and 23 M^{-1}, respectively, showing that the bathochromic shift of the absorption is also accompanied by a stronger ground-state donor−acceptor interaction.

The linear absorption spectra of the prepared polymer samples are shown in Figure 2. Both samples have almost complete extinction above 600 nm due to the presence of NPADVBB. For the sample with 2 wt % TNF, the charge-transfer absorption mainly coincides with the onset of the absorption of the dye, except in the wavelength range from 600 to 700 nm. The spectrum of the 2 wt % TNFDM-doped sample has a shoulder from 600 to 900 nm due to the charge-transfer transition. The offset in both samples is caused by reflection from the air−glass−polymer interfaces.

2. Ellipsometric Measurements. The total refractive-index modulation as a function of the frequency of the applied field was determined by ellipsometric measurements at 633 and 830 nm, as described in ref 12. Briefly, the sample is placed between crossed polarizers, an oscillating electric field of variable frequency is superimposed to a DC field, and both are applied to the sample. A linearly polarized light beam is incident on the sample under an angle of 45°. As the oscillating electric field modulates the refractive index of the sample through birefringence, Pockels effect or Kerr effect, it also modulates the relative phase of the s- and p-components of the transmitted light and hence the light intensity after the analyzer. An analysis of the intensity modulation at high and low frequency yields $\mu^2\Delta\alpha$ and $\mu\beta$, where μ is the dipole moment, $\Delta\alpha$ the polarizability anisotropy, and β the first hyperpolarizability of the nonlinear optical chromophore.

The ellipsometric response of the NPADVBB-I sample at 633 and 830 nm is shown in Figure 3. Both the fundamental response and the harmonic response are lower at 830 nm than at 633 nm. The molecular constants of NPADVBB that were determined from these curves are $\Delta\alpha(633\text{ nm}) = (2.5 \pm 0.5) \times 10^{-23}$ esu; $\Delta\alpha(830\text{ nm}) = (1.7 \pm 0.4) \times 10^{-23}$ esu; $\beta(633\text{ nm}) = (60 \pm 11) \times 10^{-30}$ esu; and $\beta(830\text{ nm}) = (43 \pm 9) \times 10^{-30}$. The decrease in the optical constants upon going from 633 to 830 nm is attributed to the dispersion in the optical coefficients as the measurement wavelength moves further away from the absorption maximum of the dye (405 nm in a NPADVBB/PVK/ECZ/TNF 39/39/20/2 wt % thin film). In a previous paper, we showed that this dispersion follows a two-level model.[13]

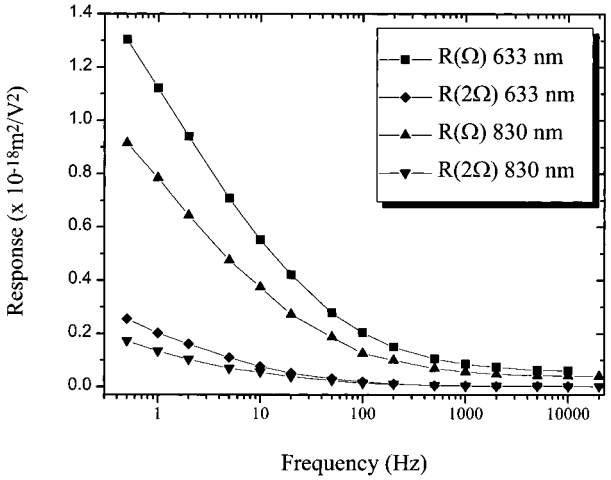

Figure 3. Ellipsometric response as a function of frequency for NPADVBB/PVK/ECZ/TNF 39/39/20/2 wt %.

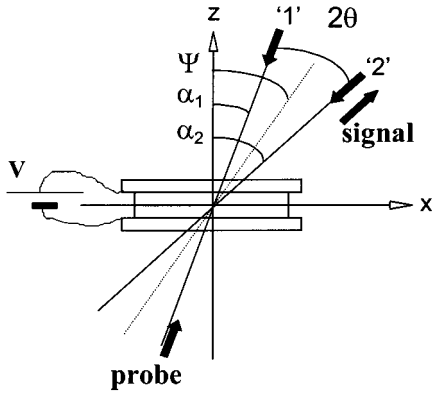

Figure 4. Geometry used in the four-wave mixing experiments.

For polymers with T_g below the measurement temperature, a possible figure of merit (FOM) for estimating the efficiency of the chromophores has been defined as[7,14,15]

$$\mathrm{FOM} = \frac{2}{9kT}\Delta\alpha\mu^2 + \beta\mu \qquad (1)$$

It is proportional to the total index modulation amplitude. The molecular constants for DMNPAA at 633 nm can be extrapolated from the values at 830 and 675 nm[12] using a two-level model to account for the dispersion and are $\Delta\alpha(633\text{ nm}) = 4.2 \times 10^{-23}$ esu and $\beta(633\text{ nm}) = 130 \times 10^{-30}$ esu. The value of the ground-state dipole moment of NPADVBB (7.4 D), however, is significantly larger than that of DMNPAA (5.5 D), which yields a slightly larger figure of merit for NPADVBB: FOM(DMNPAA, 633 nm) = 7.6×10^{-45} esu and FOM(NPADVBB, 633 nm) = 7.9×10^{-45} esu.

3. Four-Wave Mixing Measurements. The geometry used in the four-wave mixing measurements is shown in Figure 4. For the four-wave mixing experiments performed at 633 nm, the laser source was a He−

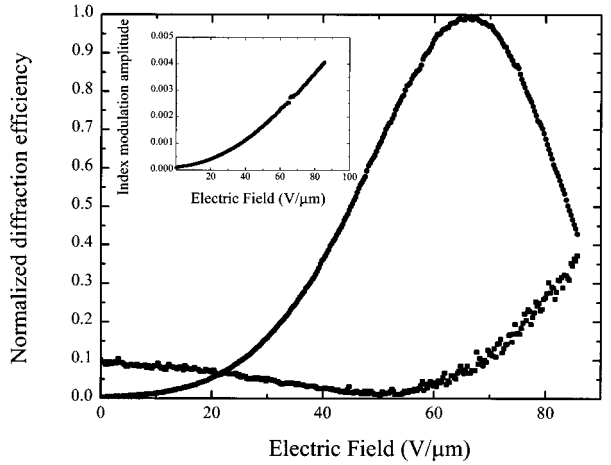

Figure 5. Normalized diffraction efficiency as a function of applied field for NPADVBB/PVK/ECZ/TNF 39/39/20/2 wt % at 633 nm, using a p-polarized (circles) and an s-polarized (squares) probe beam. The inset shows the index modulation amplitude calculated from Kogelnik's theory as a function of applied field.

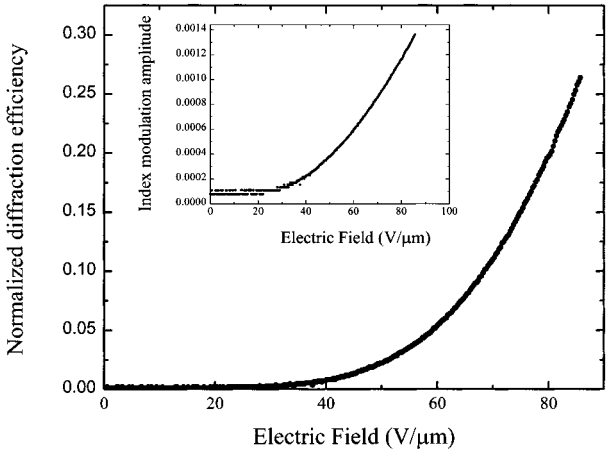

Figure 6. Normalized diffraction efficiency as a function of applied field for NPADVBB/PVK/ECZ/TNFDM 39/39/20/2 wt % at 830 nm, using a p-polarized (circles) probe beam. The inset shows the index modulation amplitude calculated from Kogelnik's theory as a function of applied field.

Ne laser. The two writing beams had a power of 1.1 mW each, were s-polarized, and were focused to spot sizes of ≈450 μm in the sample. The angle between the beams outside the sample ($2\theta_0$) was 20.5°, and the tilt angle ψ was 60°. The grating spacing under these conditions is 3.1 μm. The probe beam was either s- or p-polarized, had a power of 2.2 μW, and was focused to a spot size of ≈450 μm. The value of the externally applied electric voltage was varied from 0 to 9 kV. The refractive index of the polymer composites was measured at 633 and 830 nm using a Metricon prism coupler in substrate mode ($n_{633} = 1.72$, $n_{830} = 1.68$).

The normalized diffraction efficiency is defined as the ratio of the intensity of the diffracted beam and the intensity of the probe beam that is transmitted when no grating is being written in the sample by the writing beams. In a typical four-wave mixing experiment, the intensity of the diffracted and transmitted beams is recorded as a function of the applied electric field. Since the transmission of the sample varies slightly with electric field, a separate electroabsorption measurement is performed for an identical probe beam in the direction of the diffracted beam. The normalized diffraction efficiency is then calculated as

$$\eta_{\text{norm}} = \frac{I_{\text{diffracted,FWM}}}{I_{\text{transmitted,electroabsorption}}} \tag{2}$$

The normalized diffraction efficiency as a function of the applied electric field for sample NPADVBB-I is shown in Figure 5. For a p-polarized probe beam, nearly complete internal diffraction occurs at an electric field of 65 V μm^{-1}. The external diffraction efficiency (defined as the ratio of the diffracted intensity and the intensity of the incident probe beam, it takes into account the absorption of the polymer at 633 nm) reaches a maximum of 50% at that field strength. For an s-polarized probe beam, a diffraction efficiency of 10% is observed at zero field and is attributed to a grating formed by multiple trans/cis photoisomerization processes of the azo dye.

The normalized diffraction efficiency η_{norm} is related to the index modulation amplitude Δn by Kogelnik's coupled-wave theory in a thick medium:[16]

$$\eta_{\text{norm}} = \frac{\sin^2\sqrt{\nu^2 - \xi^2}}{\left(1 - \frac{\xi^2}{\nu^2}\right)} \tag{3}$$

with

$$\nu = \frac{\pi \Delta n d}{\lambda\sqrt{c_i c_d}} \hat{e}_i \cdot \hat{e}_d \tag{4}$$

and

$$\xi = \frac{\alpha d}{4}\left(\frac{1}{c_i} - \frac{1}{c_d}\right) \tag{5}$$

d is the sample thickness (105 μm), α is the optical absorption of the polymer ($\alpha_{633} = 66$ cm^{-1}), λ is the wavelength, and c_i and c_d are the cosines of the angle between the sample normal and the writing beams. For the geometry shown in Figure 4, the values of c_i and c_d are 0.896 and 0.837, respectively. The scalar product of the polarization vectors of the incident ($\hat{e}_i$) and diffracted ($\hat{e}_d$) beams is equal to 0.99 for a p-polarized probe beam in our experimental configuration and to 1 for an s-polarized probe beam.

Using these values, eqs 3 and 4 reduce to $\nu = 596\Delta n$ and $\xi = -0.0136$. Formula 2 can then be simplified if we assume that $\Delta n \geq 10^{-4}$. In that case $\nu^2 \geq 20\xi^2$ and $\nu^2 - \xi^2 \cong \nu^2$ or $1 - \xi^2/\nu^2 = 1$. Equation 2 then becomes

$$\eta_{\text{norm}} = \sin^2(596\Delta n) \tag{6}$$

The index modulation amplitude can be calculated from eq 6. The index modulation amplitude as a function of the applied field is shown in the inset of Figure 5. The maximum index modulation of $\Delta n = 0.0040$ occurs at an electric field of 85 V μm^{-1}.

Four-wave mixing measuments were also performed using exactly the same external angles, but with 830 nm as a working wavelength and for samples with TNFDM as a sensitizer. The grating spacing was 4.1 μm. The data in Figure 6 were recorded for s-polarized writing beams and a p-polarized probe beam. No complete diffraction occurs at this wavelength, even at

electric fields as high as 85 V μm^{-1}. Nevertheless, the normalized diffraction efficiency reaches a value of 28%. The index modulation amplitude shown in the inset of Figure 6 was calculated according to the previous procedure, but with slightly different experimental parameters ($\alpha_{830} = 40$ cm^{-1}). A maximum index modulation amplitude of $\Delta n = 0.0013$ is found at 85 V μm^{-1}.

In these materials with T_g below room temperature, the total index modulation amplitude is given mainly by the sum of the electro-optic contribution and the modulated birefringence:[7]

$$\Delta n = \Delta n_{EO} + \Delta n_{BR} \tag{7}$$

According to the oriented gas model, Δn_{EO} and Δn_{BR} can be related to the molecular constants by[17]

$$\Delta n_{BR} = \frac{2\pi}{n}\frac{2}{45}G_1 N f_\infty \Delta\alpha\left(\frac{\mu}{kT}\right)^2 E_{ext}E_{sc} \tag{8}$$

$$\Delta n_{EO} = \frac{8\pi}{n}G_2 N f_\infty f_0 \frac{\mu\beta}{15kT}E_{ext}E_{sc} \tag{9}$$

where N is the molecular number density, $f_\infty = (n^2 + 2)/3$ and $f_0 = \epsilon(n^2 + 2)/(2\epsilon + n^2)$ are the local field correction factors, E_{sc} is the space-charge field, and E_{ext} is the externally applied electric field. G_1 and G_2 depend on the experimental geometry and the polarization of the probe beam. ϵ is the static dielectric constant of the material (10). For a p-polarized reading beam G_1 and G_2 are equal to 1.01 and 1.51, respectively.[7,17]

If the values of $\Delta\alpha$ and β deduced from the ellipsometric measurements are inserted into eqs 8 and 9, we find that, for a p-polarized reading beam, $\Delta n_{BR}/\Delta n_{EO} = 2.4$ at 633 nm and $\Delta n_{BR}/\Delta n_{EO} = 2.3$ at 830 nm. At both wavelengths, the major contribution to the index modulation amplitude stems from the modulated birefringence. Since the total index modulation amplitude at both wavelengths is equal to the sum of Δn_{BR} and Δn_{EO}, it can also be verified that

$$\frac{\Delta n_{633}}{\Delta n_{830}} = 1.44\frac{(E_{sc})_{633}}{(E_{sc})_{830}} \tag{10}$$

based only on the dispersion in $\Delta\alpha$ and β and assuming equal electric field amplitudes. However, the ratio of the index modulation amplitudes calculated from the diffraction efficiencies at 633 and 830 nm is 3, which indicates that the magnitude of the space-charge field is smaller at 830 nm than at 633 nm. A possible explanation for this difference is the reduced absorption of the carbazole−TNFDM charge-transfer complex at 830 nm ($\epsilon_{830} = 61$ M^{-1} cm^{-1}, in $CHCl_3$) compared to that of the carbazole−TNF charge-transfer complex at 633 nm ($\epsilon_{633} = 250$ M^{-1} cm^{-1}, in $CHCl_3$). Because the photogeneration quantum efficiency closely follows the optical spectrum,[18] this can lead to a lower charge-generation rate and hence could explain the smaller space-charge field for the composite sensitized with TNFDM at 830 nm.

4. Two-Beam Coupling Measurements. Two-beam coupling experiments were done at 633 nm with p-polarized beams, a tilt angle ψ of 60° and an angle of 20.5° between the two beams. A general expression for

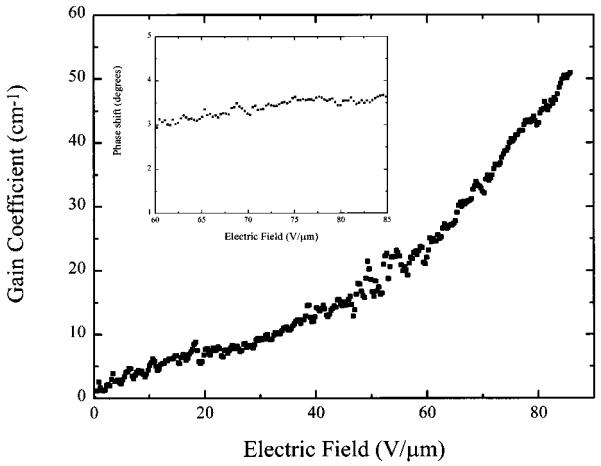

Figure 7. Gain coefficient as a function of applied field for NPADVBB/PVK/ECZ/TNF 39/39/20/2 wt % at 633 nm, using p-polarized beams. The inset shows the phase shift of the index grating, calculated from the gain coefficient and the index modulation amplitude.

Γ can be obtained from Kukhtarev's theory of dynamic self-diffraction in a photorefractive medium:

$$\Gamma d = \cos\alpha_1 \ln\left(\frac{I^t_1(I_2\neq 0)}{I^t_1(I_2=0)}\right) - \cos\alpha_2 \ln\left(\frac{I^t_2(I_1\neq 0)}{I^t_2(I_1=0)}\right) \tag{11}$$

I^t_1 and I^t_2 are the transmitted intensities of writing beams 1 and 2.[19] The gain coefficient Γ as a function of electric field is shown in Figure 7. The gain coefficient for the NPADVBB-doped composite NPADVBB-I is significantly smaller than that obtained for a similar composite doped with DMNPAA at 675 nm, 50 cm^{-1} versus 220 cm^{-1} at an electric field of 85 V μm^{-1}.

According to the coupled-wave equations, the two-beam coupling coefficient is related to both the phase shift θ between the intensity pattern and the index pattern and the index modulation amplitude:

$$\Gamma = \frac{4\pi}{\lambda}(\hat{e}_1\cdot\hat{e}_2^*)\Delta n \sin\theta \tag{12}$$

where $\hat{e}_i$ are the polarization vectors of the incoming beams. From this equation and using the index modulation amplitude from the four-wave mixing experiments, the phase shift can be calculated. Since both Δn and Γ are known with the highest accuracy in the electric field range from 60 to 85 V μm^{-1}, the phase shift was calculated only between these limits. As can be seen in the inset of Figure 7, it is a slowly increasing function of the applied field and reaches a maximum of 3.7° at an electric field of 85 V μm^{-1}.

The phase shift of the index grating with respect to the intensity pattern is a function of many parameters, such as the trap density of the photorefractive centers, and the electric field. If the only mechanism for charge transport is diffusion, the phase shift is equal to 90° according to the standard model for the photorefractive effect in inorganic crystals. For photorefractive polymers, however, a strong external electric field is necessary to obtain a large photogeneration quantum yield. The drift of mobile charges under the applied electric field is the main mechanism for charge transport and will cause the phase shift to deviate from 90°. In most of the guest−host polymer composites we have devel-

oped so far, the values reported for the phase shift almost never approached 90°. The values reported in literature are often are as small as 10−20°.[20] These small values of the phase shift are consistent with the predictions of Kukhtarev's model if one assumes large trap densities. A fit of the phase shift using the standard Kukhtarev model gives a trap density of (8.95 ± 0.03) × 10^{17} traps/cm^3. In our polymers, the density of traps can be associated with the density of photorefractive centers, that is the density of sensitizing molecules. A loading of 2 wt % of TNF leads to a density of 4.6 × 10^{19} TNF molecules/cm^3. The calculated value of 8.9 × 10^{17} traps/cm^3 is compatible with this value. While the nonzero value of the phase shift still is a signature of the photorefractive effect, its low value shows that this material is not optimized for asymmetric energy exchange, even though it has a large index modulation and diffraction efficiency. Theoretically, an identical grating, but with a phase shift of 90°, would have a coupling coefficient of $\Gamma = 800$ cm^{-1}, which shows that it is certainly possible to further improve the two-beam coupling gain.

IV. CONCLUSION

We have synthesized the chromophores NPADVBB and NPADB. Because NPADVBB is a mixture of four isomers, it has improved resistance against crystallization. Ellipsometric measurements show that NPADVBB has a FOM slightly higher than that of DMNPAA. In four-wave mixing experiments, polymer composites with NPADVBB 40 wt %, PVK/ECZ 2/1, and TNF 2 wt % showed nearly total diffraction at 633 nm. Using Kogelnik's theory, an index modulation amplitude of $\Delta n = 0.0040$ was calculated at 85 V μm^{-1}. The two-beam coupling coefficient at 633 nm was limited by the small phase shift between the index grating and the intensity pattern.

If TNF is substituted for TNFDM as a sensitizer, the spectral sensitivity of the material is extended into the infrared and a diffraction efficiency of 29% is obtained at 85 V μm^{-1}. From Kogelnik's theory and the oriented gas model, it can be calculated that the difference in diffraction efficiencies at both wavelengths is too large to be caused by dispersion in the molecular constants only, implying a smaller amplitude of the space-charge field at 830 nm in these materials.

Acknowledgment. This work was supported by the U.S. Office of Naval Research (ONR) through the Center for Advanced Multifunctional Nonlinear Optical Polymers and Molecular Assemblies (CAMP), by the U.S. National Science Foundation (NSF), by an international CNRS/NSF travel grant, by a NATO grant (900611), and by the USAF Office of Scientific Research (AFOSR) and the U.S. Ballistic Missile Defense Organization (BMDO). E.H. is a postdoctoral fellow of the Fund for Scientific Research—Flanders (Belgium). The authors would like to thank G. Guillemet and Y. J. Yao for their experimental assistance and Drs. Barzoukas and Fort (IPCMS, Strasbourg, France) for the dipole moment measurements.

References and Notes

(1) Kukhtarev, N. V.; Markov, V. B.; Odulov, S. G.; Soskin, M. S.; Vinetskii, V. L. *Ferroelectrics* **1979**, *22*, 949.
(2) Günter, P.; Huignard, J.-P. In *Photorefractive Materials and Their Applications*; Springer-Verlag: Berlin, 1988, 1989; Vols. I and II.
(3) Ducharme, S.; Scott, J. C.; Twieg, R. J.; Moerner, W. E. *Phys. Rev. Lett.* **1991**, *66*, 1846.
(4) Wiederrecht, G. P.; Yoon, B.; Wasielewski, M. R. *Science* **1995**, *270*, 1794.
(5) Lundquist, P. M.; Wortmann, R.; Geletneky, C.; Twieg, R. J.; Jurich, M.; Lee, V. Y.; Moylan, C. R.; Burland, D. M. *Science* **1996**, *274*, 1182.
(6) Meerholz, K.; Volodin, B. L.; Sandalphon; Kippelen, B.; Peyghambarian, N. *Nature* **1994**, *371*, 497.
(7) Moerner, W. E.; Silence, S. M.; Hache, F.; Bjorklund, G. C. *J. Opt. Soc. Am. B* **1994**, *11*, 320.
(8) Hendrickx, E.; Volodin, B.; Steele, D. D.; Maldonado Rivera, J. L.; Wang, J. F.; Kippelen, B.; Peyghambarian, N. *Appl. Phys. Lett.* **1997**, *71*, 1159.
(9) Meerholz, K.; Bittner, R.; De Nardin, Y.; Bräuchle, C.; Hendrickx, E.; Volodin, B. L.; Kippelen, B.; Peyghambarian, N. *Adv. Mater.* **1997**, *9*, 1043.
(10) Cox, A. M.; Blackburn, R. D.; West, D. P.; King, T. A.; Wade, F. A.; Leigh, D. A. *Appl. Phys. Lett.* **1996**, *68*, 2801.
(11) Foster, R. in *Organic charge-transfer complexes*; Academic Press: New York, 1969.
(12) Sandalphon; Kippelen, B.; Meerholz, K.; Peyghambarian, N. *Appl. Opt.* **1996**, *35*, 2346.
(13) Sandalphon; Wang, J. F.; Kippelen, B.; Peyghambarian, N. *Appl. Phys. Lett.* **1997**, *71*, 873.
(14) Kippelen, B.; Meyers, F.; Peyghambarian, N.; Marder, S. *J. Am. Chem. Soc.* **1997**, *119*, 4559.
(15) Wortmann, R.; Poga, C.; Twieg, R. J.; Geletneky, C.; Moylan, C. R.; Lundquist, P. M.; DeVoe, R. G.; Cotts, P. M.; Horn, H.; Rice, J. E.; Burland, D. M. *J. Chem. Phys.* **1996**, *105*, 10637.
(16) Kogelnik, H. *Bell Syst. Tech. J.* **1969**, *48*, 2909.
(17) Kippelen, B.; Meerholz, K.; Peyghambarian, N. In *Nonlinear Optics of Organic Molecules and Polymers*; Nalwa, H. S., Miyata, S., Eds.; CRC Press, Inc.: Boca Raton, FL, 1997; p 482.
(18) Andre, B.; Lever, R.; Moisan, J. Y. *Chem. Phys.* **1989**, *137*, 281.
(19) Volodin, B. L.; Sandalphon; Meerholz, K.; Kippelen, B.; Kukhtarev, N. V.; Peyghambarian, N. *Opt. Eng.* **1995**, *34*, 2213.
(20) Silence, S. M.; Scott, J. C.; Stankus, J. J.; Moerner, W. E.; Moylan, C. R.; Bjorklund, G. C.; Twieg, R. J. *J. Phys. Chem.* **1995**, *99*, 4096.

MA9714777